An investigation on the adsorption behavior of Sb (III) on a cationic ion exchange resin in Fixed-bed column: experimental design and breakthrough curves modeling

F. Moghimi [1], H. Yoozbashizadeh [2,*], A. H. Jafari [3], M. Askari [2]

[1] Department of Materials Engineering, Science and Research Branch, Islamic Azad University, Tehran, Iran
[2] Sharif University of Technology Department of Materials Science & Engineering, P.O. Box 11155-9466, Tehran, Iran
[3] Shahid Bahonar University of Kerman, Department of Materials Science and Engineering, College of Engineering, Kerman, Iran

ARTICLE INFO

Article history:

Received 8 January 2020
Accepted 13 May 2020
Available online 15 September 2020

Keywords:

breakthrough curve
Bohart-Adams model
Thomas model
Yan model
Elution
Saturation Time

ABSTRACT

The purpose of this study is to investigate and optimize parameters effective on continuous adsorption and elution and study of the corresponding breakthrough curve models for the removal of one of the main pollutants found when copper is extracted and refined. Mining has a long history of producing toxic waste so there is a heightened sense of urgency for finding ways to protect the environment especially during the initial production stages. The contaminants in water and mine wastewater are key issues in the reuse of water resources. In this study, adsorption by fixed-bed column which is usually applied for removing organic contaminants from the aqueous phase is investigated for adsorption of the antimony on a commercially available cationic resin Purolite S957 and the kinetics of adsorption is explored by establishing breakthrough and resin saturation times. Concentration and feed flow rate affect the kinetics of adsorption on a fixed-bed resin and were determined both experimentally as well as through optimization by a two-level factorial experimental design using Central Composite Design (CCD). Experiments were carried out at constant temperature and pH of 55 ℃ and 8 respectively that were determined based on optimal conditions for fixed resin content of 25 g. The breakthrough test results suggest Bohart-Adams model better fitted the experimental data compared to Thomas and Yan models with R^2 of 0.964. Moreover, elution of pure antimony occurred at 15 BV of elution solution and maximum concentration of antimony was achieved at about 300 $mg.L^{-1}$

1-Introduction

Antimony (Sb) is a toxic metalloid that has become a global environmental problem due to Sb-mining activities. The toxicity and mobility of Sb strongly depend on its chemical speciation [1]. Lately, it has aroused the interest of many researchers due to its toxicity and to the varied industrial and commercial applications of its compounds [2]. Among various alloy-based materials, Sb is a promising anode material for KIBs with a high theoretical capacity of 660 mA.h g^{-1} [3].

* Corresponding author:
E-mail address: yoozbashi@sharif.edu

lead-acid batteries, semiconductor components, flame proofing materials, glass, pigments, and catalysts are other uses of this metalloid. The main source of Sb pollution is mining activities, which generate waste waters contaminated by Sb(III) or/and Sb(V) [4,5] with the trivalent form being more toxic [6,7]. Sb is an impurity found in copper refining electrolyte which must be removed. The traditional treatment of Sb has a number of disadvantages such as loss of high-value copper in a low-value recycling product[8]. Adsorption in fixed-bed columns has many advantages due to its simple operation and higher efficiency. The design of fixed-bed column optimization involve mathematical models that are used for the description and prediction of the experimental data of the breakthrough curves [9,10]. The region of the bed where the absorption process occurs is called the mass transfer zone (MTZ) or the absorption region or active region [11]. The performance of packed beds is evaluated through the concept of the breakthrough curve, where time for appearance of adsorbate in flowing stream and the shape of curve it takes are important characteristics for determining the dynamic response of a resin. The position of the breakthrough curve along the volume axis depends on the capacity of the column with respect to the feed concentration and flow rate. Ideally, the breakthrough curve would be a step function, in other words, there would be an instantaneous jump in the effluent concentration from zero to the feed concentration at the moment the column capacity is reached [12, 13]. Three kinetic models including Adams-Bohart, Thomas, and Yoon-Nelson models are used to assess experimental data to predict the breakthrough curves and to determine the characteristic parameters of the column [14]. The mathematical modeling, if correctly undertaken, could play a key role in the scale-up procedures from laboratory experiments through pilot plant to industrial scale with minimum of time and expense. It can help to analyze and explain experimental data, identify mechanisms relevant to the process, predict changes due to different operating conditions, and to optimize the overall efficiency of the process. Mathematical breakthrough curve models have been used to predict a fixed-bed column performance and also to calculate kinetic constants and uptake capacities [15]. Three analytical breakthrough curve models were employed to fit the experimental data: Thomas, Bohart-Adams, and Yan models. The Thomas model which is widely used to evaluate the column performance can be employed to predict the the maximum solute uptake by the adsorbent. It assumes that the adsorption rate obeys the pseudo-second-order, Langmuir equation, and no axial dispersion in the column. The model can be expressed as follows:

$$C_t/ C_o = 1/1+\exp(K_{th}/Q(q_{TH}.W- C_o.Q.t)) \quad (1)$$

where k_{TH} is the Thomas model rate constant (mL min^{-1} mg^{-1}) and q_{TH} is the theoretical saturated adsorption capacity (mg. g^{-1}). The model developed by Bohart and Adams in 1920 is commonly applied to the initial stage of the breakthrough curve. This model relies on the assumption of the step isotherm, with the capacity of setting the adsorbent to a constant value [16]. This model is expressed as:

$$C_t/ C_o = \exp (K_{BA}. C_o)/\exp (K_{BA}.N_0.Z/v)- 1+\exp(K_{BA.} C_o.t) \quad (2)$$

where k_{BA} is the Bohart-Adams model rate constant (mL. min^{-1} mg^{-1}), N_0 is the uptake volumetric capacity (mg L^{-1}), *Z* is the bed height (cm), and *v* is the linear flow rate (cm min^{-1}), which is calculated by Eq. (9):

$$V=Q/A \quad (3)$$

where Q is the flow rate (mL min^{-1}) and A is the column cross section area (cm^2).

The Yan model or modified dose-response was proposed in order to minimize the error that results from the use of the Thomas model, especially at very small and very large operation times. This model can be formulated as follows [17]:

$$C_t/ C_o = 1-1/1+(C_o.Q.t/q_y.W)a_Y \quad (4)$$

where q_Y is the amount of solute adsorbed (mg. g^{-1}) and a_Y is the constant of Yan model. Software design is based on a scientific method for statistical analysis of results of pre-planned tests so that the obtained data have some accepted level of certainty.

Central composite design (CCD) is the most common response surface method (RSM) used for estimating the coefficients of a second-order model. The method covers certain groups of design points, namely factorial design points, surface with fractional factorial, axial points, and central points. Purolite S597 resin used in this research is a general-purpose commercial absorbent of the phosphonate-mono phosphonic containing phosphoric and sulfonic acid [18], and was studied for continuous adsorption of Sb in flow mode and to analyze the breakthrough curves from kinetic perspectives using the models of Thomas, Bohart-Adams, and Yan. Fixed-bed column system was evaluated in laboratory scale through a two-level factorial experimental design and the effectiveness of the model to predict influences of initial Sb concentration and volumetric flow rate on breakthrough and saturation times, the volume of effluent treated, and fractional bed utilization were utilized for design of the resin column. Riveros et al. [19] report an effective method to elute Sb(V) from the amino-phosphonic resins, which are used industrially to control the Sb concentration in copper electrolytes. Sb(V) is extremely difficult to elute from amino-phosphonic resins, thus, in industrial practice, a gradual build-up of Sb(V) often takes place on the resin beads, leading to a reduction in the resin capacity and useful life. Thiourea addition reduces Sb(V) to Sb(III), a reaction that can only take place in concentrated HCl. This work examines optimization of the adsorption mechanism and also elution through validation of modeling results with experimental data as a way of designing efficient non-stop flow removal of antimony and prevention of Sb(IV) formation.

2- Materials and methods

2-1- Reagents

The Sb sulfate of analytical grade and 99.99% purity was supplied from Sigma-Aldrich Company (Missouri, USA).

2-2- Fixed bed column studies

2-2-1- Experimental procedure

Atomic adsorption spectroscopy (AAS) analysis of industrial copper refinery electrolyte for Sb content is given 0.35 $g.L^{-1}$ and was used as the basis for the formulation of antimony sulfate and iron sulfate solutions made using Sigma analytical grade compounds as shown in Table 1.

Fixed-bed experiments were carried out using a 25 mm diameter, 50 cm long borosilicate glass column, the bottom of which was filled with 5 mm thick glass wool, to acted as resin storage In this process, wastewater enters the bed directly and passes through the bed by its gravity. The bed was filled with 25g resin and to ensure temperature stability, the container was setup in a water bath equipped with a heater and thermostat. A diaphragm pump continually circulates the electrolyte from a 10 liter container of Sb sulfate solution of 0.35 $g.L^{-1}$ concentration which was uniformly diffused from the 5-mm thick glass wool on the bead column. To ensure repeatability of the results they were, carried out-at least three times. For each test, a definite volume 10 BV or 250 mL of column outflow was sampled and cation concentration was measured using atomic absorption spectroscopy (AAS). Elution tests were performed utilizing 500 mL of hydrochloric acid of different concentrations at different flow rates and temperatures on the Sb-adsorbed resin bed.

Table 1. Metallic salts to make synthetic solution specimens.

Chemical name	**Chemical Formula**	**Purity**	**Formula weight**	**Salt Concentration** $g.L^{-1}$	**Ion concentration** $g.L^{-1}$	**Manufacture ID**
Antimony (Sb) sulfate	$Sb_2(SO_4)_3$	99.99%	531.707	1.31	0.35	10783 Sigma

2.2.2. Surface response experimental design methods

Tests were set up based on the central composite design (CCD), using Design Expert software to determine the effects of significant experimental parameters such as response—time to achieve 95% initial concentration (t_s), time to achieve 5% of initial concentration or concentration progress (t_b), volume of treated solution (Vs), and fraction of bed used (FBU). The primary variables of initial concentration of Sb (C_o) and flow rate (Q) were selected based on previous works [17] and the results of tests determining the range of responses in the present research. Summary of data of input parameters and range of variation in real and software-encoded formats is presented in Table 2. The elution tests were carried out for investigating the effect of HCl concentration, temperature, and flow rate on the concentration of Sb after elution as the response ,

$$q_s = C_o\, Q/1000W \int_0^{ts} (1- Cs/ C_o) \quad (5)$$

$$q_s = C_o\, Q/1000W \int_0^{ts} (1- Cs/ C_o) \quad (6)$$

$$C_b = 0.05\, C_o \quad (7)$$

$$C_s = 0.95\, C_o \quad (8)$$

$$V_s = t_s\, Q/W \quad (9)$$

$$FBU = q_b/q_s \quad (10)$$

where C_o, C_b, and C_s are the initial, breakthrough, and saturation concentration of Sb (mg L^{-1}), respectively. t_b and t_s are the breakthrough and saturation time (min), Q is the flow rate (mL. min^{-1}), W is the weight of adsorbent in the column, and q_b and q_s are the amount of Sb adsorbed at breakthrough and saturation time (mg. g^{-1}), respectively. Ten tests with different values of input parameters were performed. The values of responses are shown in Table 3. For elution, 18 tests with different values of input parameters were performed. The values of the responses are summarized in Table 4.

Table. 2. Summarized information of variables in actual and software-encoded formats based on CCD

Encoded Values		Maximum	Minimum	Unit	Parameter
1 (350)	-1 (100)	40.77	48.22	$mg.L^{-1}$	C_o
1 (6)	-1 (2)	6.84	1.17	$mL.min^{-1}$	Q

Table. 3. Table of design containing information of tests and response values.

Run	C_o	Q	t_s	t_b	V_s	FBU
	$mg.L^{-1}$	$mL.min^{-1}$	min	min	$mL.g^{-1}$	-
1	225	4	437.5	129.5	62.5	5.42
2	100	6	661.5	349	141.74	10.28
3	350	6	188.5	126	40.39	12.7
4	225	1.17	1508	119.57	63.09	15.27
5	350	2	1000	689	80	8.47
6	100	2	1966.5	1654	140.46	16.07
7	225	6.82	259.12	73.2	63.11	0.53
8	225	4	442	125	63.14	5.4
9	48.22	4	2047	1734	292.42	16.14
10	401.77	4	244	62.5	34.85	5.2

Table 4. Table of elution design containing information of tests and response values for elution

Run	T (C)	HCl Concentration (M)	Q_e (mL.min^{-1})	C_{Sb} (gL^{-1})
1	45	4.5	3	0.15
2	60	7.0	2	0.31
3	45	4.5	3	0.19
4	30	7.0	2	0.20
5	45	4.5	3	0.15
6	45	4.5	3	0.15
7	60	2.9	2	0.14
8	19	4.5	3	0.02
9	30	7.0	4	0.10
10	30	2.0	4	0.03
11	45	8.0	3	0.25
12	60	7.0	4	0.30
13	70	4.5	3	0.18
14	45	0.2	3	0.05
15	45	4.5	3	0.15
16	60	2.0	4	0.10
17	45	4.5	3	0.15
18	45	4.5	1	0.18

3. Results and Discussion

3.1. ANOVA analysis for adsorption Responses

A reliable way to check the quality of data compliance is using analysis of variance (ANOVA). Association between output responses (i.e., t_s, t_b, v_s, and the fraction of bed used (FBU)) and input variables (i.e., initial concentration of Sb (C_o), and flow rate (Q)) was suggested through reduced quadratic polynomial equations and transfer functions based on encoded variables as follows.

$1/t_s$= 277.2e-03.0+272.1e-003.0 A+131.1e-003.0B+298.6e-004.0AB (11)

t_b= 75.127-86.498 A-38.377 B+25.295 AB+49.342 A2+04.211 B^2 (12)

1/(V_s)= 016.0+911.8E-003.0 A-364.3E-005. B+715.8E-005.0 A^2 (13)

FBU=24.8-22.4 A-44.4 B (14)

In Eqs. (11) and (13), the inverse transfer function was used for modeling the experimental data. The ANOVA results are presented in Table 5. As can be seen, the responses of the models are at 95% confidence level suggesting that model coefficients have p-values less than 0.05. Higher ratios of mean squares regression to residual (F) suggest a desirable regression of experimental data [20]. For instance, for p-value of 0.0041 and F-value of 24.79 for the response t_b in Table 5 indicate the significance and suitability of the selected model. Lack of fit test is used to review the observations that were not taken into account in the choice of model. In order to support this, the high value of p and the low value of F are required [21]. In the same vein, p-value and F-value (i.e., 0.8497 and 0.35, respectively) suggest non-significance of the test for the response Vs. Since p-values greater than 0.1 are statistically insignificant, all model terms with p-values higher than 0.1 were excluded. As a result, no significant correlation was found between input variables of Vs and FBU responses.

Table. 5 ANOVA results for adsorption Responses.

Source	Sum of Squares	Mean Square	F Value	p-value Prob > F
ts	2.475×10^{-5}	8.250×10^{-6}	32709.77	0.0001<
C_o	$1.293x\ 10^{-5}$	$1.293x\ 10^{-5}$	51285.91	0.0001<
Q	$1.023x\ 10^{-5}$	$1.023\ x\ 10^{-5}$	40552.07	0.0001<
C_o * Q	$1.587\ x\ 10^{-6}$	$1.587\ x\ 10^{-6}$	6291.33	0.0001<
Residual	$1.513x\ 10^{-9}$	$2.522x10^{-10}$		
Lack of Fit	$1.242\ x\ 10^{-9}$	$2.485\ x\ 10^{-10}$	0.92	0.6556
Pure Error	$2.708\ x\ 10^{-10}$	$2.708x10^{-10}$		
Total	$2.475\ x10^{-5}$			
t_b	$4.038\ x10^{6}$	$8.076\ x\ 10^{5}$	24.79	0.0041
C_o	$1.991\ x\ 10^{6}$	$1.991\ x\ 10^{6}$	61.11	0.0014
Q	$1.139\ x\ 10^{6}$	$1.139\ x\ 10^{6}$	34.97	0.0041
C_o * Q	$3.487\ x\ 10^{5}$	$3.487\ x\ 10^{5}$	10.70	0.0307
$C_o^{\ 2}$	$5.362\ x\ 10^{5}$	$5.362\ x\ 10^{5}$	1646	0.0154
Q^2	$2.036\ x\ 10^{5}$	$2.036\ x\ 10^{5}$	6.25	0.0668
Residual	$1.133\ x\ 10^{5}$	32580.66		
Lack of Fit	$1.133\ x\ 10^{5}$	43437.50	4290.12	0.0112
Pure Error	10.13	10.13		
Total	$4.169\ x\ 10^{6}$			
Vs	$6.352\ x\ 10^{-4}$	$2.117\ x\ 10^{-4}$	35330.98	0.0001<
C_o	$6.352\ x\ 10^{-4}$	$6.352\ x\ 10^{-4}$	$1.060\ x\ 10^{-5}$	0.0001<
Q	$9.053\ x\ 10^{-9}$	$9.053\ x\ 10^{-9}$	1.51	0.2651
C_o^2	$4.253\ x\ 10^{-8}$	$4.253\ x\ 10^{-8}$	7.10	0.0373
Residual	$3.596\ x\ 10^{-8}$	$5.993\ x\ 10^{-9}$		
Lack of Fit	$1.315\ x\ 10^{-8}$	$4.562\ x\ 10^{-9}$	0.35	0.8497
Pure Error	$1.315\ x\ 10^{-8}$	$1.315\ x\ 10^{-8}$		
Cor Total	$6.353\ x\ 10^{-4}$			
FBU	217.07	108.54	17.73	0.0030
C_o	119.64	119.64	19.54	0.0045
Q	132.38	132.38	21.62	0.0035
Residual	36.73	1.12		
Lack of Fit	36.73	7.35	36731.22	0.0040
Pure Error	$2.000\ x\ 10^{-4}$	$2.000\ x\ 10^{-4}$		
Total	253.80			

The statistical propositions supporting regression of experimental data for all four responses are presented in Table 6. The close-to-one values of the R-squared (R^2), adjusted R-squared (adj- R^2), and predicted R^2 show that there is a consistency between experimental data and estimations [22]. For instance, the R^2 value of the modeled t_s (i.e., 0.9687) suggests that more than 96.87% of experimental data is describable through this model [23]. On the other hand, the parameters coefficient of variance, (C.V%)

and adequate precision in Table 6 indicate the ratio of the standard deviation to mean and the ratio of signal to noise. Here, the desirable responses are those with C.V% values less than 4 and adequate precision higher than 4 [24]. The parameter "PRESS", which refers to the sum of predicted squares of residuals, is detailed in Tables 7 and 8. Lower values of the parameter are recommended because they lead to the lower error of the model and higher regression share [25]. Fig. 1 shows whether residuals of ten runs of Table 3 follow normal probability and distribution diagram. The results of all responses suggest that the distribution of residuals is linear, which supports the normal distribution of system errors.

Table. 6 Statistical parameters calculated from the regression of experimental responses of models (a) t_s, (b) t_b, (c) Vs, and (d) FBU.

a (t_s)			
Std. Dev.	1.588×10^{-5}	R^2	0.9999
Mean	2.277×10^{-3}	Adj-R^2	0.9999
C.V. %	0.70	Pred-R^2	0.9999
PRESS	3.619×10^{-7}	Adeq Precision	480.911
b (t_b)			
Std. Dev.	180.50	R2	0.9687
Mean	570.07	Adj-R2	0.9297
C.V. %	31.66	Pred-R2	0.7777
PRESS	9.267×10^{-5}	Adeq Precision	13.136
c (Vs)			
Std. Dev.	7.742×10^{-5}	R2	0.9999
Mean	0.016	Adj-R2	0.9999
C.V. %	0.49	Pred-R2	0.9999
PRESS	9.217×10^{-8}	Adeq Precision	514.743
d (FBU)			
Std. Dev.	2.47	R2	0.8553
Mean	9.20	Adj-R2	0.8070
C.V. %	26.90	Pred-R2	0.6729
PRESS	83.03	Adeq Precision	10.463

C.V: Coefficient of variation

Std. Dev.: Standard deviation

PRESS: Predicted residual sum of squares

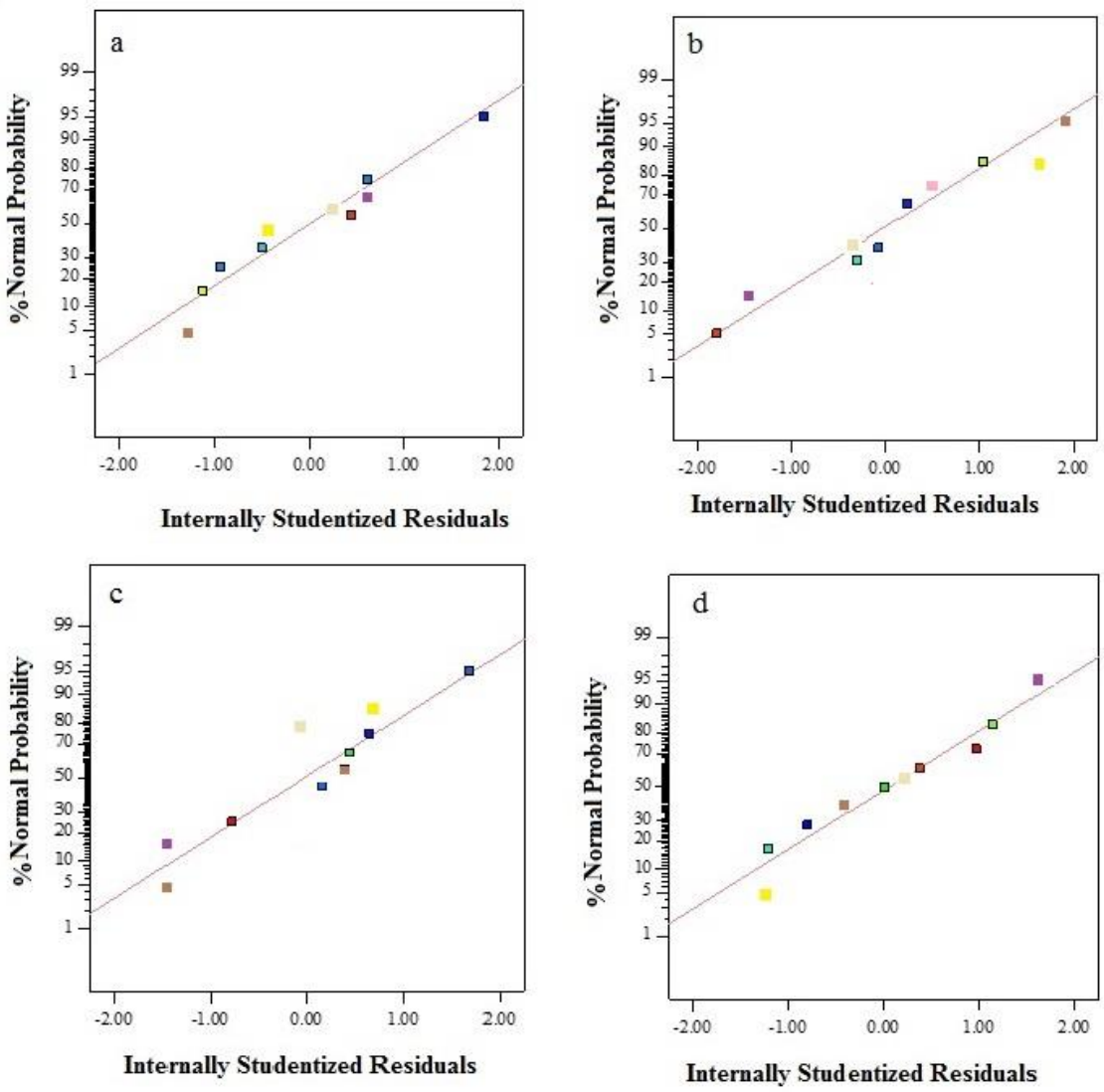

Fig. 1. Normal diagrams of residuals for responses (a) t_s, (b) t_b, (c) V_s, and (d) FBU in a continuous system. colors shows residuals of ten runs of Table 3 that(Run1, Run2, Run3, Run4, Run5 , Run6 , Run7, Run8, Run9, Run10).

The diagram of internally normalized residual based on estimated values is represented in Fig. 2. The expected response is a random distribution and this behavior is found for all responses [26]. Variation of responses t_b, t_s, V_s, and FBU as a function of simultaneous variations of the variables C_o and Q (flow rate) are presented in the three-dimensional diagrams shown in Fig. 3a through 3d. Fig. 3a shows the variation of response t_s, An increase in C_o and Q resulted in decreases in t_s, due to effective and rapid filling up of attractive sites at high values of initial concentration (C_o), i.e. quick saturation of the colum but, the flow rate has a negative correlation with saturation time. Therefore, time to achieve saturation is reduced by an increase in the flow rate. Moreover, at higher flow rates, the time of fluid retention in the column is not long enough such that ions leave the column before absorption

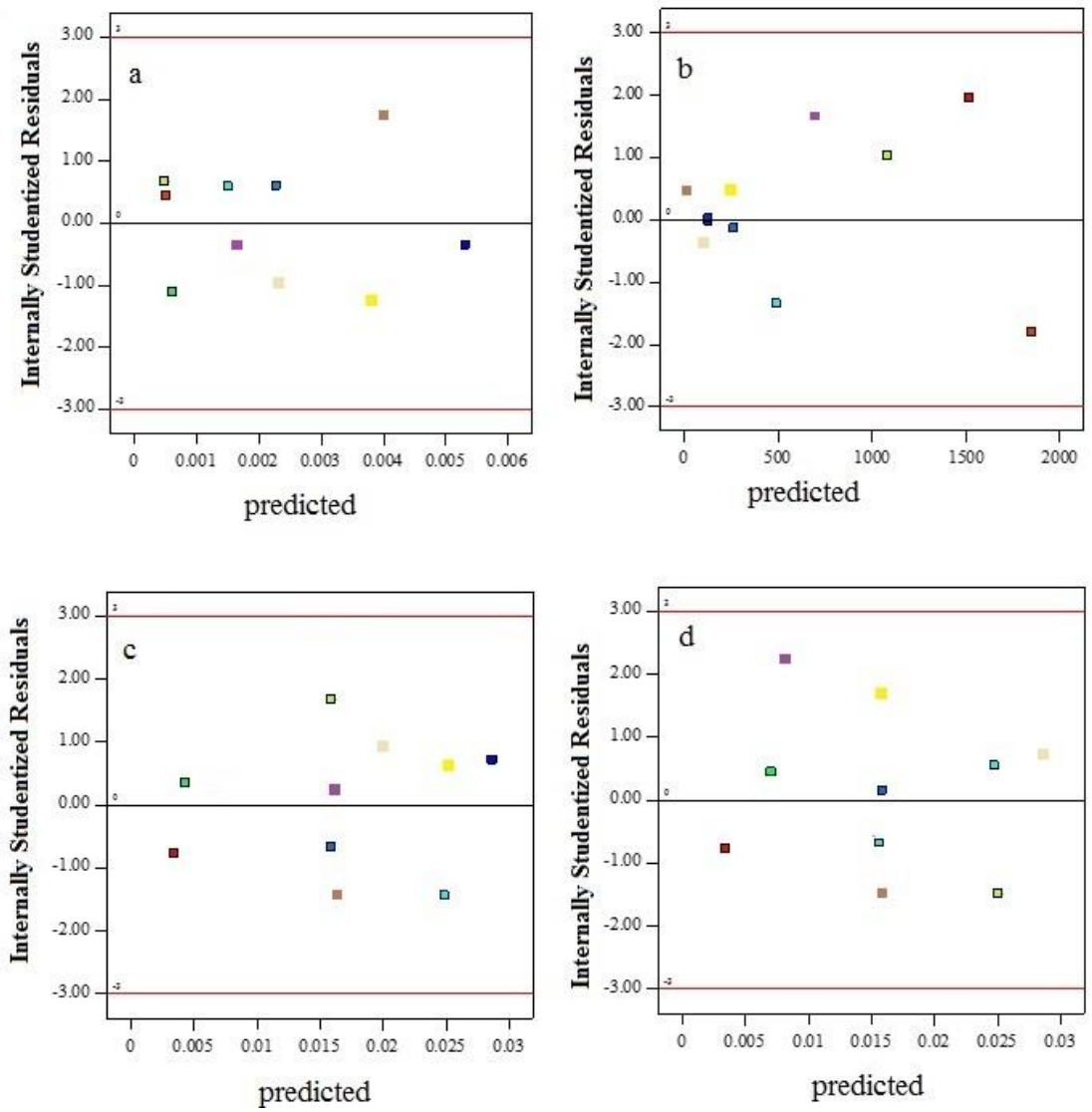

Fig. 2. Internally normalized residuals based on estimated values of the model for responses t_s (a), t_b (b), V_s (c), and FBU (d) The red lines represent Allowed range for residuals.

Fig. 3b shows the variation of response t_b. As the figure suggests, the effect of C_o on response is significant because an increase in the variable results in significant change in the response. In contrast, an increase in Q results in a reduced response due to the fact that as the flow rate rises, fluid retention time drops, leading to shorter breakthrough times at higher flow rates. Green diagrams shown in Fig. 3a and Fig. 3b are contour diagrams showing the simultaneous effect of two factors C_o and Q thatWith the simultaneous increase both t_s,t_b decrease.

According to Fig. 3c, the response Vs signifies its independence of the parameter Q. In fact, response Vs is only a function of initial concentration (C_o) as a decline of C_o is followed by a gradual increase in Vs. Initial concentration exerts a negative effect on the volume of treated wastewater because due to shallow concentration gradient, the low inflow slows down transfer of ions from the outer layer to the adsorbent surface. In this case, the penetration rate declines and does not provide the driving force for mass transfer. Fig. 3d shows the variation of FBU, the fraction of the column used for adsorption follows variations of input variables of the

linear model (Eq. 4). An increase in C_o and Q reduces FBU because the higher concentration of absorbable ions is associated with higher adsorption rate, thus, a lower fraction of the column being used in the adsorption process. Therefore, the increase in the flow rate exerts a negative effect on the adsorption rate. A low flow rate contributes to higher values of FBU also because of the reduction in the thickness of adsorption film enhances the mass transfer. Green diagrams shown in Fig. 3c and Fig. 3d are contour diagrams showing the simultaneous effect of two factors C_o and Q thatWith the simultaneous increase both Vs, FBU decrease. Table 7 shows the optimization conditions of intended variables based on average results of repetition of each new test. Comparison of the values estimated by the model and experimental results obtained under optimal conditions indicates that the model is capable of describing the studied responses.

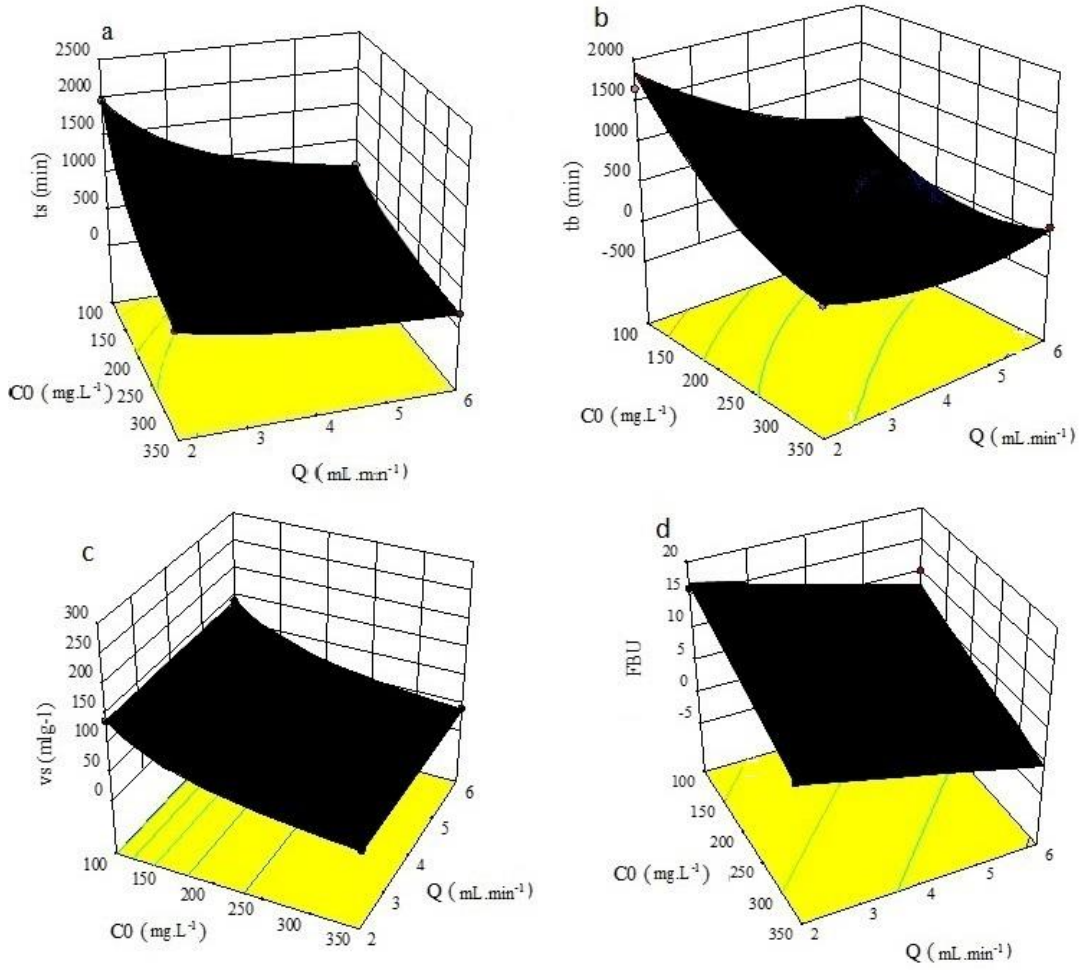

Fig. 3. Three-dimensional diagrams of the responses (a) t_s, (b) t_b, (c) Vs, and (d) FBU and simultaneous variations of C_o and Q.

Table. 7. Evaluation of model under optimal conditions for adsorption.

Test	C_o (mg.L^{-1})	Q (mL.min^{-1})		T_b (min)	T_s (min)	V_s (mLg^{-1})	FBU
11	120	2.2	Model	1500.25	1521.74	782.117	15.7797
			Test	1505	1560	800	14.5

3-3- ANOVA analysis for elution Response

The association between output responses and input variables of elution determined was suggested through the reduced quadratic polynomial equation as follows:

C_{Sb}=15.0+055.0 A+071.0 B-018.0C+003.0 AB+03.0 A^2+005.0 B^2 (15)

The ANOVA results are presented in Table 8. As can be seen, the response of the models are at 95% confidence level suggesting that model coefficients have p-values less than 0.05. Higher ratios of mean squares regression to residual (F) suggest a desirable regression of experimental data. The statistical propositions supporting regression of experimental data for response are presented in Tables 9. The close-to-one values of the R-squared (R^2), adjusted R-squared (adj- R^2), and predicted R^2 show that there is a consistency between experimental data and estimations. The elution of Sb-containing resin by HCl results in the formation of chloroanionic complexes in HCl medium but their structure is completely different. The chloro complexes are small for three-valence Sb and have high load densityAs shown in Fig. 4, the increase in HCl concentration and temperature contributes to the increase of Sb concentration from elution. At higher temperatures, elution occurs better because ion exchange is controlled by permeation into the resin matrix. As temperature rises, the viscosity of the solution drops and the penetration of exchangeable ions increases, therefore, the elution rate increases linearly as temperature rises and elution occurs better. Higher concentration of HCl is correlated with formation of the chloroanionic complexes with significant level of hydration, enhancing the elution. At lower flow rates(Q_e) and longer elution times, elution occurs better because the time of retention in the column is longer. Therefore, HCl solution leaves the column after elution of adsorbent molecules is complete. Green diagrams shown in Fig. 4a are contour diagrams showing the simultaneous effect of two factors HCl concentration and temperature thatWith the simultaneous increase both to the increase of Sb concentration. Green diagrams shown in Fig. 4b showing the simultaneous effect of two factors Q_e and temperature thatWith the increase to temperature and decreas flow ratesQ_e the increase of Sb concentration. Green diagrams shown in Fig. 4a showing the simultaneous effect of two factors HCl concentration and Q_e thatWith the increase to HCl concentration and decreas flow ratesQ_e the increase of Sb concentration

Table. 8. ANOVA results for elution.

Source	Sum of Squares	Mean Square	F Value	p-value Prob > F
Model	0.11	0.012	42.67	<0.0001
temperature	0.36	0.036	126.47	<0.0001
concentration HCl	0.059	0.059	206.73	<0.0001
Q_e	926.5e-003	926.5e-003	19.88	0.0012
Residual	832.2e-003	832.2e-003		
Lack of Fit	499.1e-003	499.1e-003	1.12	0.4505
Pure Error	333.1e-003	333.1e-003		

Table. 9. Statistical parameters extracted from the regression of experimental data of elution.

Std. Dev.	0.017	R^2	0.9799
Mean	0.15	Adj-R^2	0.9599
C.V. %	11.55	Pred-R^2	0.8385
PRESS	0.018	Adeq Precision	24.424
C.V: Coefficient of variation Std. Dev.: Standard deviation PRESS: Predicted residual sum of squares			

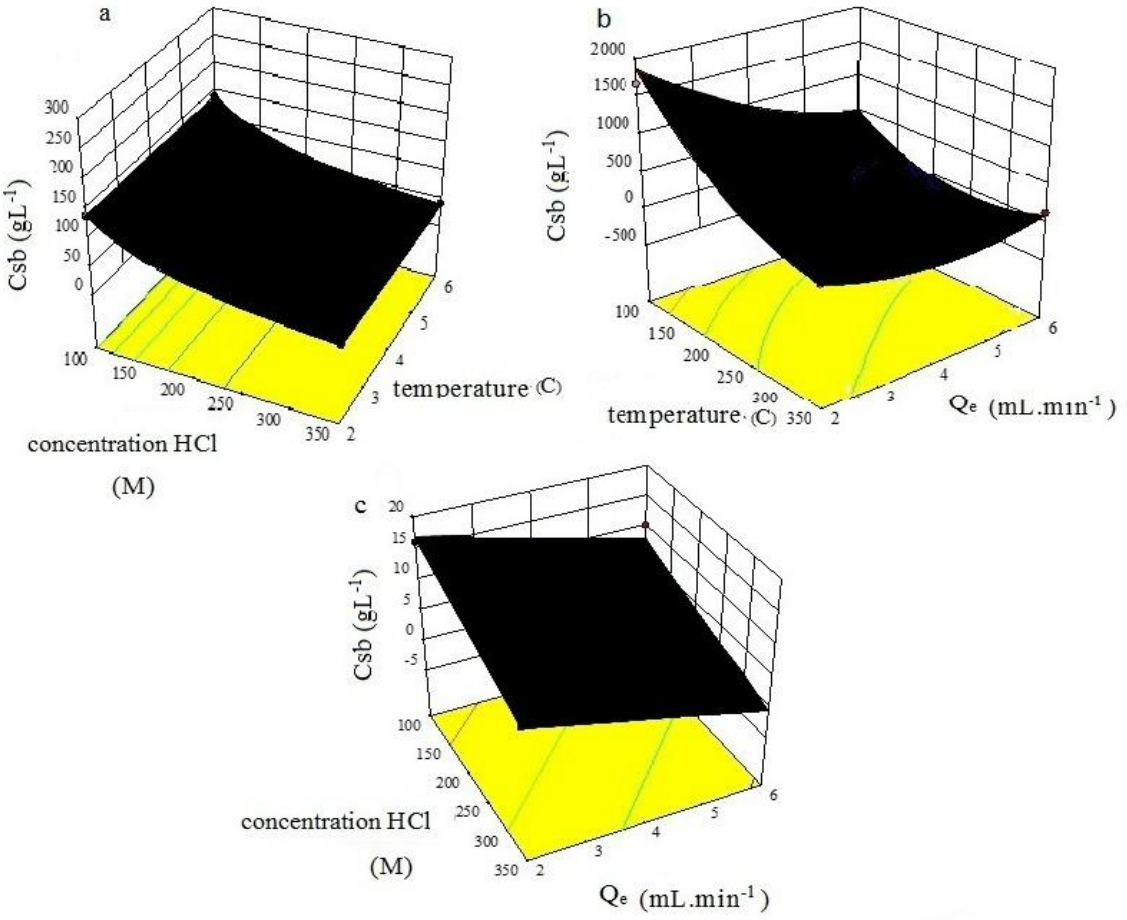

Fig. 4. Three-dimensional response as a function of (a) HCl concentration and temperature, (b) flow rate and temperature, and (c) flow rate and HCl concentration.

Table10 shows the optimization conditions of intended variables based on average results of repetition of each new test for resin elution . Fig. 5 suggests that complete elution of pure Sb occurs in 15BV of elution solution and maximum concentration of Sb is achieved at about 300mg.L^{-1}. Fig. 5 suggests that complete elution of pure Sb occurs in 15BV of elution solution and maximum concentration of Sb is achieved at about 300mg.L^{-1}. Fig. 6 indicates that longer time is associated with better elution such that within 11 hours, 65% of Sb is reduced while 97% of Sb is reduced after 18 hours.

Table. 10. Optimal conditions for resin elution by HCl Acid.

Run	HCl Concentration (M)	Q_e (mL.min^{-1})	Temperature (C°)	C_{Sb}
2	7	2	60	0.31

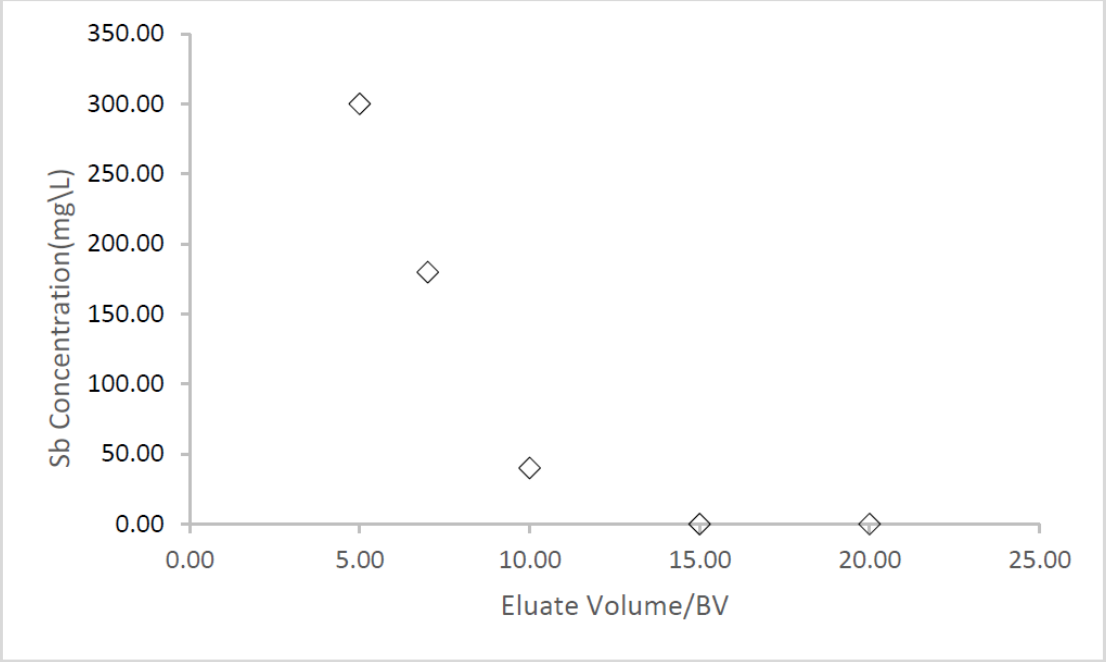

Fig. 5. Elution of Sb(III) in Purolite S957 resin under optimal conditions (initial resin load: 0.35mg.L^{-1}).

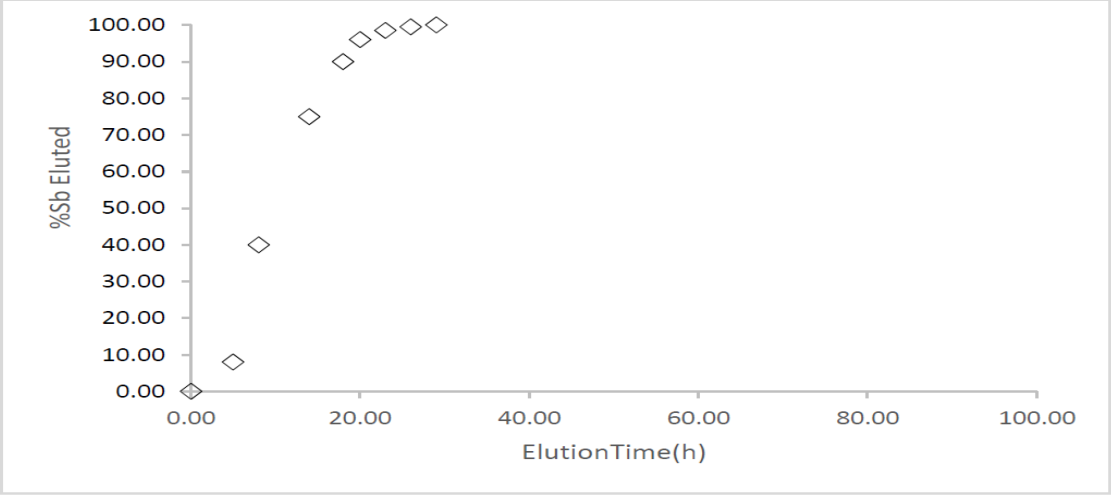

Fig. 6. Elution rate curve, Sb of resin using hydrochloric acid.

3-2- Mathematical modeling of the breakthrough curves in adsorption

Traditional analytical models of Thomas, Bohart-Adams, and Yan were employed to fit the breakthrough experimental data under different operation conditions of the experimental design. Parameters of the models are shown in Table 11. Both Thomas and Yan models are used to describe processes in which the external diffusion and Bohart-Adams model shows that intraparticle adsorption process[27].Based on the obtained results, the Bohart-Adams model is suitable to reproduce the initial behavior of the breakthrough curve. The model was satisfactorily employed with a mean R^2 of 0.962. Although this model provides a simple and comprehensive approach to run and evaluate adsorption-column tests, its validity is limited to the range of conditions applied [28,29]. Among the three models tested, the Thomas model showed the lowest average R^2 (i.e., 0.931) and Bohart-Adams model showed the highest R^2 (i.e., 0.962). The breakthrough curve of Sb at optimal conditions and the comparison between the adjustments to Thomas, Bohart-Adams, and Yan models are shown in Fig. 7.

Table 11. Thomas, Bohart-Adams, Yan models parameters for Sb by Resin on the fixed- bed column.

Model	Parameters	
Thomas model	q_{TH} (mg. g^{-1}) K_{TH} (mL .min^{-1} .mg^{-1}) R^2	0.7899 0.1099 0.931
Bohart-Adams model	K_{BA} (mL.min^{-1}.mg^{-1}) N_0 ((mg L^{-1}) R^2	1.872 0.2708 0.962
Yan model	a_y q_y (mg .g^{-1}) R^2	3 0.5539 0.9442

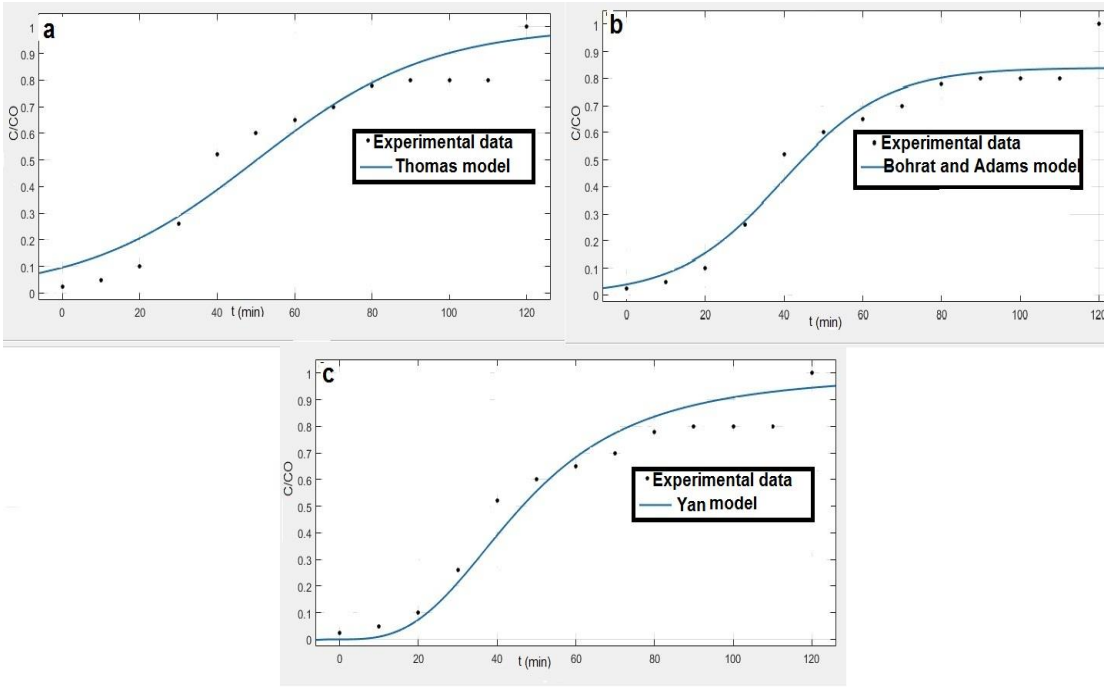

Fig. 7. The breakthrough curve of Sb adsorption onto resin in the fixed-bed column for (a) Thomas model (b) Bohrat and Adams model, and (c) Yan model.

Bohart-Adams model provides a better fit of the breakthrough curve compared to Thomas model [30]. All these results are based on using Bohrat-Adams model, which can relate batch adsorption with the fixed-bed column behavior. Sb adsorption onto resin showed to be a very favorable process at the beginning, because of high adsorbate, an adsorbent affinity, and a large number of available binding sites.

4-Conclusion

1. In this study, a set of tests were carried out on a synthesized sample solution containing pure antimony (Sb). The results suggest that in the continuous system, an increase in C_0 (i.e., the initial concentration of Sb) and Q (flow rate) is followed by lower responses of breakthrough time, saturation time, treated wastewater and fraction of bed used.

2. Complete elution of pure Sb is realized at 15 BV of elution solution.

3. Mathematical models for the breakthrough curves were successfully applied. Bohart-Adams model best fitted the experimental data of all tests ($R^2 = 0.962$).

References

[1] MENGCHANG H, NINGNING W. Antimony speciation in the environment: Recent advances in understanding the biogeochemical processes and ecological effects. 2019,75:14-39.

[2] MINGYI R, SGIMING D. Seasonal antimony pollution caused by high mobility of antimony in sediments: In situ evidence and mechanical interpretation.2019,367:427-436.

[3] CHUNHUA H, KANG H, XUANPENG W**.** Three-dimensional carbon network confined antimony nanoparticle anodes for high-capacity K-ion batteries.2018,10:6820-6828.

[4] BARKHORDAR B, GHIASSEDDIN M. Comparision of Langmuir and Freundlich Equilibriums in Cr, Cu and Ni Adsorption by Sargassum. Iran J Environ Health SciEng, 2004, 1:58–64.

[5] NABIZADEH R, NADDAFI K, SAEEDI R, MAHVI AH, VAEZI F, YAGHMAEIAN K, NAZMARA S. Kinetic and equilibrium studies of Lead and Cadmium biosorption from aqueous solutions by sargasum spp biomass. Iran J Environ Health Sci Eng, 2005, 2:159–168.

[6] UNGUREANU G, SANTOS S, BOAVENTURA R, BOTELHO C. Arsenic and antimony in water and wastewater: Overview of removal techniques with special reference to latest advances in adsorption. Journal of Environmental Management, 2015, 151:326-342.

[7] LIANG H.C. Trends in mine water treatment. Mining Magazine, 2014,66: 83-85.

[8] SUNDAR S, CHAKRAVARTY J. Antimony Toxicity. Int J Env Res Pub He, 2010, 7: 4267-4277.

[9] MITSUNOBU S.Antimony(V)incorporation into synthetic ferrihydrite goethite and natural iron oxyhydroxides. Environmental Science Technology, 2010, 44: 3712-3718.

[10]JLUIS S, RODRIGUEZ A, ALVAREZ S, GARCIA J. Analysis and modeling of fixed-bed column operations on flumequine removal onto activated carbon: pH influence and desorption studies. Chemical Engineering Journal, 2013,228: 102-113.

[11] ARROYO F,RUIZ I,GONZA L. Optimizing operating conditions in an ionexchange column treatment applied to the removal of Sb and Bi impurities from an electrolyte of a copper electro-refining plant. Hydrometallurgy, 2017, 171: 285-297.

[12] XIAO F, CAO J.M D, SHEN X. Biosorption of antimony xyanions by brown seaweeds batch and column studies.Journal of Environmental Chemical Engineering, 2017,5(4): 3463-3470.

[13] AKSU Z, GONEN F, DEMIRCAN Z. Biosorption of chromium(VI) ions by Mowital®B30H resin immobilized activated sludge in a packed bed: comparison with granular activated carbon. Process Biochem,2002,38:175–86

[14] ZUMRIYE A, FERDA G. Biosorption of phenol by immobilized activated sludge in a continuous packed bed: prediction of breakthrough curves. 2004,39:599-613

[15] ZHONG K., WANG Q. Optimization of ultrasonic extraction of polysaccharides from dried longan pulp using response surface methodology. arbohydr. Polym, 2010,80 (1): 19-25

[16] ANDREA E, FRANCO M, BONFANTE D, CARVALHO C, MARQUES BONETTO M. Removal of antimony from water by adsorption onto activated carbon in batch process and fixed-bed column: Kinetics, isotherms, experimental design and breakthrough curves modeling.Journal of Cleaner Production, 2017:1-33

[17] CHIAVOLA A, DAMATO E. Ion exchange treatment of groundwater contaminated by arsenic in the presence of sulphate. Breakthrough experiments and modeling. Water Air and Soil Pollut,2012,223(5): 2373–2386.

[18] IZADI A, AMIRI M, IZADI N.Removal of iron ions from industrial copper raffinate and electrowinning electrolyte solutions by chemical precipitation and ion exchange. Minerals Engineering, 2017,113: 23–35.

[19]RIVEROSP.The removal of antimony from copper electrolytes using aminophosphonic resins: Improving the elution of pentavalent antimony. Hydrometallurgy,2010, 105:110-114.

[20] SENTHILKUMAR R,VIJAYARAGHAVAN K, THILAKAVATHI M . Seaweeds for the remediation of wastewaters contaminated with zinc(II) ions. J. Hazard. Mater, 2006, 136(3):791–799.

[21]KHAKPOUR H, HAGHGOO M,ETEMADI K. Analysis and optimization of viscosity of concentrated silica suspensions by response surface methodology (RSM): Control of particle modality. Journal of Dispersion Science and Technology, 2017**:**1-8

[22]CHIENG B , IBRAHIM N, AND YUNUS W.W. Optimization of tensile strength of poly (lactic acid)/graphene nanocomposites using response surface methodology. Polymer-Plastics Technology and Engineering**,**2012,51 (8)*:* 791-799

[23]HASHEMI M, SHOJAOSADATI S, RAZAVI S, MOUSAVI S. Different catalytic behavior of α-amylase in response to the nitrogen substance used in the production phase. J. Ind. Eng. Chem,2015, 21*:* 772-778

[24]MAJUMDER A, SINGH A, GOYAL A. Application of response surface methodology for glucan production from Leuconostoc dextranicum and its structural characterization. Carbohydr. Polym**,** 2009 ,75 (1): 150-156

[25]BEZERRA M. A, SANTELLI R, OLIVEIRA E, VILLAR E. P, ESCALEIRA L. S. Response surface methodology (RSM) as a tool for optimization in analytical chemistry. Talanta**,**2008**,**76- (5)*:* 965-977

[26]CANDIOTI L. V, DE ZAN M. M, CAMARA M. S, GOICOECHEA H. C. Experimental design and multiple response optimization. Using the desirability function in analytical methods development. Talanta**,**2014**,**124:123-138

[27]LIAO P, ZHAN Z, DAI J, WU X, ZHANG W, WANG, K, YUAN S. Adsorption of tetracycline and chloramphenicol in aqueous solutions by bamboo charcoal: A batch and fixed-bed column study. Chem. Eng. J, 2013,228: 496–505.

[28] CALERO M, HERNAINZ F, BLAZQUEZ G, TENORIO G. Study of Cr (III) biosorption in a fixed-bed column. J. Hazard. Mater, 2009,171(1–3): 886–893

[29] SONG J, ZOU W, BIAN Y, SU F, HAN R. Adsorption characteristics of methylene blue by peanut husk in batch and column modes Desalination. 2011,265(1–3): 119–125

[30] MENG M, FENG Y, ZHANG M, LIU Y . Highly efficient adsorption of salicylic acid from aqueous solution by wollastonite-based imprinted adsorbent: A fixed-bed column study. Chem. Eng. J, 2013,225:331–339